INELASTIC ANALYSIS OF SEMIRIGID FRAMEWORKS

Y. Liu[1], L. Xu and D.E. Grierson
Civil Engineering, University of Waterloo, Canada

Abstract

This article presents an efficient method for inelastic analysis of semirigid planar steel frameworks. A compound element comprised of a plastic-hinge element and a semirigid connection element is located at member ends that may potentially undergo inelastic deformation. Nonlinear inelastic flexural behaviour is modeled by an empirical relation between moment and rotation for which the parameters are available from experimental results. A four-parameter model is employed to simulate the nonlinear moment-rotation behaviour of semirigid connections. The member stiffness matrix involving the compound element is expressed explicitly in terms of stiffness degradation factors that vary depending on the loading level. This permits direct account for the combined influence of inelastic and nonlinear connection behaviour on structure stiffness. A semirigid steel portal frame is analyzed to illustrate the proposed analysis method, and the results are compared with those obtained from experiments involving the same frame.

Keywords: semirigid connection, inelasticity, compound element

1. Introduction

Many studies have been devoted to developing practical methods of nonlinear analysis accounting for both semirigid connections and member plastic behaviour (Ziemian *et al* 1992; Chen *et al* 1994; Yau *et al* 1994; Chen *et al* 1996). However, little work has been done to investigate the interaction between the behaviour of semirigid connections and that of member plasticity. This study focuses on such interaction using the concept of a compound element, which is shown in Figure 1 and explained in detail in the following.

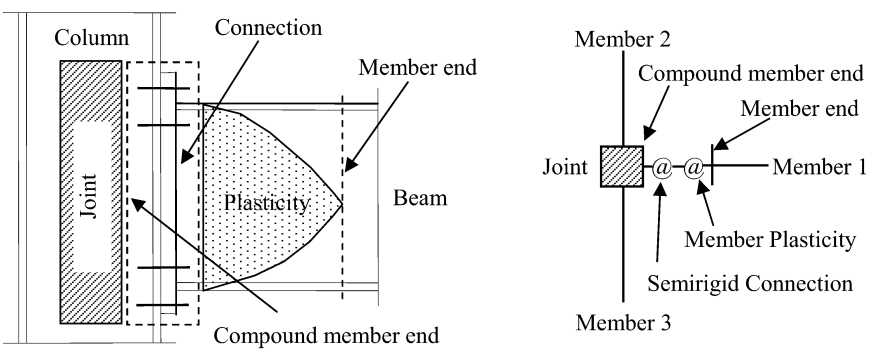

(a) Actual connection and plasticity (b) Analytical model

Figure 1. Connection and inelasticity model at a joint

Figure 1(a) is a typical beam-to-column connection joint involving member plasticity. Typically, the connection is semirigid and possibly includes bolts, welds and angles. The member plastic zone forms at the beam end due to concentrated internal loads. To facilitate nonlinear analysis, Figure 1(a)

[1] Corresponding author: Y27liu@uwaterloo.ca

M. Pandey et al. (eds), Advances in Engineering Structures, Mechanics & Construction, 317–328.

may be replaced by the analytical model shown in Figure 1(b), where one of the two springs represents the plasticity formed at the member end while the other spring represents the semirigid connection.

A method of analysis has been recently developed by the authors to deal with geometric and material nonlinearities (Grierson *et al* 2005, Xu *et al* 2005). The goal of this article is to extend this method to account for semirigid connections using a so-called compound-element approach. At each stage of the analysis, the combined-stiffness degradation due to semirigid connection and member plasticity behaviour is determined, and the corresponding tangent stiffness matrix for the structure is formed. The process ends when the specified external loads are completely applied on the structure or the limit loading state is reached.

2 Rotational Compound Element

This section uses the series theorem to develop a compound element representing the combined rotational stiffness behaviour of a semirigid connection together with a member-end plastic hinge. The determination of the stiffness of semirigid connections is discussed in detail, while that for member-end plasticity is adopted directly from the authors' previous research (Grierson *et al* 2005, Xu *et al* 2005).

2.1 Series Element Model

The series element model involves a semirigid connection spring, an inelastic spring and an elastic member all connected in series. The nature of the compound element is indicated in Figure 2, where parameters R_n, R_e, R_c, R_p denote the rotational stiffnesses of the compound member end, elastic member end, semirigid connection spring, and the member plasticity spring, respectively. Only end 1 of the member is considered, while end 2 may or may not have the same nature as end 1.

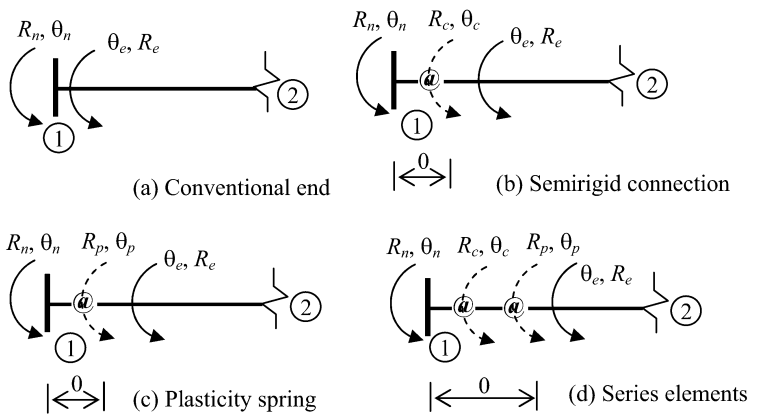

Figure 2. Compound-rotational element at the member end

The case in Figure 2(a) is conventionally used in structural analysis, where a beam-to-column connection at node 1 is assumed as either a pinned connection ($R_n = 0$) or fixed connection ($R_n = R_e$). This assumption makes analysis and design simple both for hand and computer-based analysis. However, if the effect of actual connections on structural responses must be considered, the model of the semirigid connection shown in Figure 2(b) is introduced in the analysis and design of structures. Another case is also popular in rigid-plastic analysis, where a plastic hinge is abruptly formed rather than gradually degrading from initial yield to full yield states. To improve the accuracy in this latter method, the inelastic model shown in Figure 2(c) is used to model the property of the gradual stiffness degradation due to the presence of plasticity. Finally, if both semirigid connection and plasticity behaviour may occur at the same time, the series-element model shown in Figure 2(d) should be introduced in analysis and design, as in the work of Yau and Chan (1994) where, however, the influences of plasticity and semirigid connections were considered separately. To facilitate structural

analysis accounting for both connection and inelasticity stiffness degradations and their interactions, an integrated compound element is needed and is investigated in detail as follows.

The rotational deformation involving nonlinear connection and inelasticity behaviour indicated in Figure 2(d) is graphically represented in Figure 3(a) using two springs. It can be verified that the two series-connected springs may be substituted by the compound element shown in Figure 3(b) involving a single spring. The compound stiffness R that reflects the combined stiffnesses R_c and R_p can be derived as in the following (Liu 2005).

Provided that a moment M is applied at the joint in Figure 3(a), the relative rotations θ_c and θ_p are given by,

$$\theta_c = M / R_c;\ \theta_p = M / R_p \tag{1}$$

Since the total relative rotation θ between the joint and the elastic member end is the summation of rotations induced by the connection and inelastic springs, from Eqs (1) the rotation θ can be expressed as,

$$\theta = \theta_c + \theta_p = M / R_c + M / R_p = M / R \tag{2}$$

where the compound rotational stiffness,

$$R = \frac{1}{1/R_c + 1/R_p} = \frac{R_c R_p}{R_c + R_p} \tag{3}$$

accounts for both connection and plasticity stiffness.

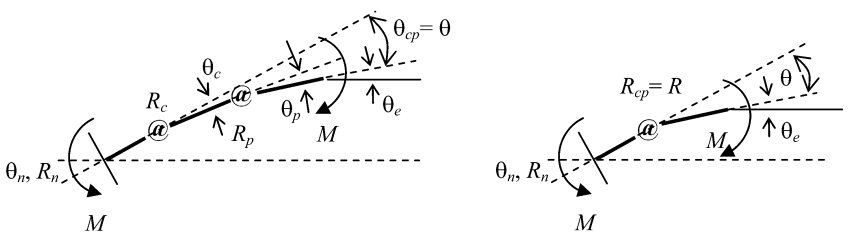

Figure 3. Simplified compound member-end model

2.2 Determining stiffness R_c

It remains to determine the stiffness of the compound element through Eq. (3). The inelastic stiffness R_p of the member is directly available in the literature (Grierson *et al* 2005). Thus, only the connection stiffness R_c in Eq. (3) need be established herein.

Several semirigid connection models have been proposed (Xu 1994), and of these models the four-parameter power model, originally proposed for modeling the post-elastic stress-strain relation (Richard *et al* 1975), is commonly used in analysis. Recently, this model has been further confirmed to be effective and accurate for predicting the behaviour of end-plate connections on the basis of experimental data for extended-end-plate and flush-end-plate connections (Kishi *et al* 2004). Thus, the following four-parameter model,

$$M = \frac{(R_{ce} - R_{cp})\theta_c}{\left\{1 + [(R_{ce} - R_{cp})\theta_c / M_0]^{\gamma}\right\}^{1/\gamma}} + R_{cp}\theta_c \tag{4}$$

is employed in this study to simulate the behaviour of semirigid connections. In Eq. (4), θ_c denotes the relative rotation of the semirigid connection, and the four parameters R_{ce}, R_{cp}, M_0, and γ are the initial rotation stiffness, strain-hardening/softening stiffness, reference moment, and shape parameter of the

connection, respectively. The initial yield moment M_{cy} and corresponding rotation θ_{cy} determine the elastic stiffness $R_{ce}= M_{cy}/\theta_{cy}$, while the reference moment M_0, strain-hardening/softening stiffness R_{cp}, and rotation capacity θ_u determine the ultimate moment capacity to be,

$$M_u = M_0 - \theta_u R_{cp} \tag{5}$$

where the rotation capacity θ_u depends on the connection type and can be determined from the results of existing research (e.g., Bjorhovde *et al* 1990). The four parameters in Eq. (4) can be found for different types of connections from an existing database of experimental results (Xu 1994).

Differentiating Eq. (4) with respect to rotation θ_c determines the tangent stiffness of the connection to be (Richard *et al* 1975),

$$R_c = \frac{dM}{d\theta_c} = R_{cp} + \frac{R_{ce} - R_{cp}}{\left\{1 + [(R_{ce} - R_{cp})\theta_c / M_0]^{\gamma}\right\}^{1+1/\gamma}} \tag{6}$$

where R_{ce} is the elastic rotational stiffness at the initial condition $\theta_c = 0$, while R_{cp} is the strain-hardening/softening stiffness when rotation θ_c tends to infinity (for practical steel structures, θ_c can reach at most to the limiting rotation capacity of the connection when fracture occurs (Bjorhovde *et al* 1990).

It is seen from Eqs (4) and (6) that the four-parameter model reduces to a linear model with $R_c = R_{ce}$ when R_{cp} tends to R_{ce} , whereas a bilinear model is reached when the shape parameter γ approaches to infinity. If R_{cp} is set to zero (i.e., strain-hardening/softening is ignored), Eq. (4) reduces to the following three-parametric model that was previously suggested by Kishi and Chen (1987),

$$M = \frac{R_{ce}\theta_c}{[1 + (R_{ce}\theta_c / M_u)^{\gamma}]^{1/\gamma}} \tag{7}$$

where the reference moment M_0 is replaced by the ultimate moment M_u. Note that the rotation θ_c can be explicitly obtained from Eq. (7) as,

$$\theta_c = M / R_{ce}[1 - (M / M_u)^{\gamma}]^{1/\gamma} \tag{8}$$

Using an expression for post-elastic rotation previously derived by the authors (Grierson *et al* 2005, Xu *et al* 2005), and the connection rotation given by Eq. (8), the total relative rotation θ of the compound element can be explicitly expressed as,

$$\theta = \frac{M}{R_{ce}[1 - (M / M_u)^{\gamma}]^{1/\gamma}} + \phi_p \left\{1 - \left[1 - \left(\frac{M - M_y}{M_p - M_y}\right)^{\alpha}\right]^{1/\alpha}\right\} \quad \frac{M_y}{M_p} \le \frac{M}{M_p} \le 1 \tag{9}$$

which represents the moment-rotation relationship of the compound element. The benefit of using the three-parameter model is that the rotation θ_c of the connection is directly obtained in the nonlinear analysis for the given moment M; the disadvantage is that the strain-hardening or softening nature of the connection is omitted. In contrast, strain hardening/softening is accounted for in the four-parameter model, but an iterative procedure is needed to find the relative rotation θ_c of the connection. Both of the connection models are considered for the verification analysis presented later.

2.3 Degradation Factors

The flexural stiffness degradation factor associated with the semirigid stiffness R_c is given by (Monforton *et al* 1963),

$$r_c = 1/(1 + 3EI / LR_c) \tag{10}$$

where EI/L is the flexural stiffness of the elastic member. The factor r_c is interpreted as the ratio of the end rotation of the elastic member to the combined rotation of the elastic member and the connection due to unit end-moment (Xu, 1994).

Similarly, the stiffness degradation factor associated with the inelastic stiffness R_p is given by (Grierson *et al* 2005),

$$r_p = 1/(1 + 3EI / LR_p) \tag{11}$$

where the factor r_p is interpreted as the ratio of the inelastic rotation M/R_p to the total elastic and inelastic rotation $M/R_p + ML/3EI$ under the action of bending moment M applied at the end connected to the compound element in the case when the far end of the elastic member is simply supported (Xu *et al* 2005).

To evaluate the combined stiffness effect, a stiffness degradation factor associated with the compound stiffness R is introduced and similarly expressed as $r = 1/(1+3EI/LR)$. The factor r is the ratio of the rotation of the compound element to the sum total of the rotation of the compound element plus the rotation of the elastic member when simply supported at the far end. From Eqs (3), (10) and (11), the compound stiffness degradation factor is found as,

$$r = \frac{1}{1 + 3EI / LR_c + 3EI / LR_p} = \frac{r_c r_p}{r_c + r_p - r_c r_p} \tag{12}$$

which maps $R \in [0, \infty]$ to $r \in [0, 1]$. From Eq. (12), the stiffness degradation factor for the compound element is a function of the degradation factors of the semirigid connection and member inelasticity, such that if any of these factors degrades to zero then the stiffness of the compound element will degrade to zero as well.

3 Characteristics of Compound Rotational Element

The behaviour of the compound rotational element is dependent upon the strength capacities of the connection and the connected beam members. For the current study, the effect of connected columns on the behaviour of the beam-column connection is ignored and the shear deformation of panel zones is not considered.

If considering only the effect of member plasticity, the moment-rotation relation in the post-elastic range is as shown in Figure 4(a), whereas when considering the effect of the semirigid connection alone the moment-rotation relationship is as shown in Figure 4(b). In Figure 4, M_u is the ultimate moment capacity of the connection, while M_y and M_p are the initial-yield and fully-plastic moment capacities of the connected member, respectively. Depending on the interaction of member inelasticity and nonlinear connection behaviour, three types of semirigid connections may be characterized by the compound element, as described in the following.

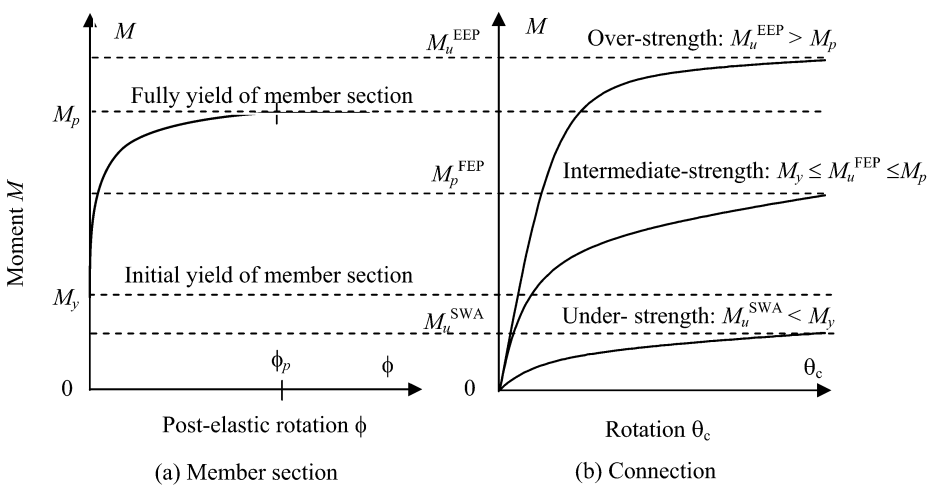

Figure 4. Stiffness-degradation relationship at a member end

(1) Under-strength connections: $M_u < M_y$

In this situation, the performance of the compound element is governed purely by the semirigid connection, and no inelasticity occurs in the vicinity of the member end. This may occur for single web-angle (SWA) connections with $M_u = M_u^{SWA}$. The combined moment-rotation behaviour of the compound element is shown in Figure 5, which is exactly the semirigid behaviour shown in Figure 4(b). This kind of connection is referred to as an Under-strength connection since the strength capacity of the compound element is less than the yield strength of the member. If M_u is small enough or the rotational constraint is ignored, this type of connection is categorized as a conventional simple or pinned connection (AISC 2001, CISC 2004).

(2) Intermediate-strength connections: $M_y \le M_u \le M_p$

In this second case, both the semirigid connection and member inelasticity govern the behaviour of the compound element, but the limit strength is determined by the nature of the connection. Such behaviour of the compound element may occur for a flush end-plate (FEP) connection. This type of connection is referred to as an intermediate-strength connection and corresponds to a partially restrained (AISC 2001) or semirigid (CISC 2004) connection.

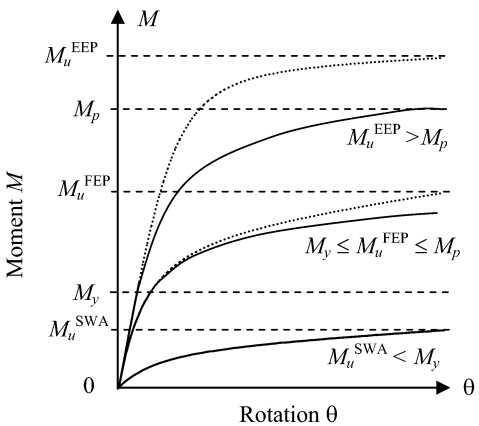

Figure 5. M-θ relations of compound

(3) Over-strength connections: $M_p < M_u$

Finally, when the ultimate moment of the connection is greater than the plastic moment of the connected member, and even though the connection influences the stiffness degradation of the compound element due to its nonlinear behavior, the member inelasticity dominates the behaviour of the compound element. An example for an extended end-plate (EEP) connection is illustrated in Figures 4 and 5 (where the dotted moment-rotation curve refers to the EEP connection considered alone). It can be seen from Figure 5 that the moment-rotation behaviour of the compound element (solid curve) is dominated by the plastic capacity of the member. This kind of connection is referred to as an over-strength connection and corresponds to a fully restrained (AISC 2001) or rigid (CISC 2004) connection (i.e., in the limit when the connection stiffness is considered infinite).

It can be seen from the foregoing discussion that a satisfactory design may be achieved if both the connection and the corresponding connected member have the same strength capacity, i.e., $M_p = M_u$. It is not good to use an over-strength connection, i.e., $M_u > M_p$, since the over-strength of the connection is not utilized in any way. Lower-strength connections may be used in circumstances where stiffeners can be added to avoid excessive deformation.

In the common case of a pinned connection, i.e., $r_c = 0$, the compound element has zero rotational stiffness regardless of the value of r_p. In this case, any connected member does not experience plastic behaviour. If $r_c = 1$, the compound element behaviour is determined by the inelastic behaviour of the member, i.e., $r = r_p$ in the case of a rigid connection. It is noted that when the plasticity factor is

smaller than unity (e.g., $r_p = 0.7$), the r value of the compound element is close to the value of r_c (Liu 2005). This means that even if the member end has experienced some plasticity (e.g., 100-70 = 30%), the stiffness of the compound element is dominated by the connection. In other words, the level of inelasticity has insignificant effect on the stiffness degradation of the compound element. If the ultimate strength of a connection is close to, or lower than, the initial yield strength of the connected member, the influence of member plasticity on structural response may be ignored.

4 Structural Analysis

Once the stiffness degradation factor of a compound element is determined, as discussed in the previous sections, the structural analysis is readily conducted. This study focuses planar steel frameworks comprised of beam-column members with compact sections, for which plastic deformation is not precluded by local buckling (AISC 2001). The plastic bending, shearing or axial deformation (ϕ, γ or δ) of a member under the action of moment, shear or axial force (M, V or P) is concentrated at a member-end section (Xu *et al* 2005). Figure 6(a) shows a general member with Young's modulus E, shear modulus G, member length L, cross-section moment of inertia I, sectional area A, and equivalent shear area A_s. The parameters R_{pj}, T_{pj} and N_{pj} are respectively the post-elastic rotational bending, transverse shearing and normal axial stiffness of the member at the two end sections j =1, 2, while R_{cj}, T_{cj} and N_{cj} are respectively the rotational bending, transverse shearing and normal axial stiffness of the connections at the two end sections. Upon adopting a compound element at each member-end, the simplified model shown in Figure 6(b) is obtained, where the determination of the corresponding parameters is discussed in the following.

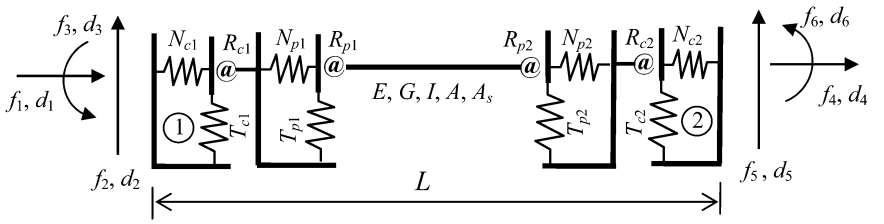

(a) Elements in series

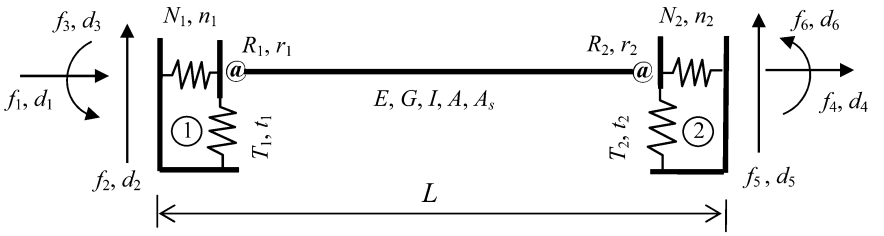

(b) Compound elements

Figure 6. Beam-column-member model used in analysis

The evaluation of connection and member rotational stiffnesses R_{cj} and R_{pj} in Figure 6(a), and corresponding stiffness degradation factors r_{cj} and r_{pj} , has been discussed in detail in the previous sections. The member transverse shear and normal axial stiffnesses T_{pj} and N_{pj} were determined in previous research, where it was shown that the corresponding stiffness degradation factors t_{pj} and n_{pj} are given by (Grierson *et al* 2005, Xu *et al* 2005),

$$t_{pj} = 1/(1+3EI/L^3T_{pj})\,;\; n_{pj} = 1/(1+EA/LN_{pj}) \tag{13a, b}$$

which map T_{pj} or $N_{pj} \in [0, \infty]$ into t_{pj} or $n_{pj} \in [0, 1]$. Similarly, the transverse and normal stiffness degradation factors for the connection can be expressed as,

$$t_{cj} = 1/(1+3EI/L^3T_{cj})\,;\; n_{cj} = 1/(1+EA/LN_{cj}) \tag{14a, b}$$

where T_{cj} and N_{cj} are the transverse shear and normal axial stiffnesses of the connection.

In this study, it is assumed that: 1) the transverse shear stiffness T_{cj} or normal axial stiffness N_{cj} of a connection is infinite when the materials are in the elastic range, and that the corresponding degradation factor t_{cj} or n_{cj} in Eqs (14) is unity; and 2) the stiffness T_{cj} or N_{cj} is zero when the materials are in the plastic range, and that the corresponding degradation factor t_{cj} or n_{cj} is zero. Such idealized perfectly elastic-plastic models are shown in Figure 7.

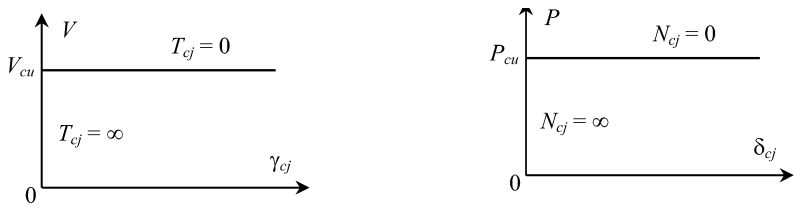

(a) Transverse case (b) Normal case

Figure 7. Idealized shear & axial force-displacement relations for connections

Upon determining the parameters characterizing the compound element, the general planar compound member shown in Figure 6(b) is generated, where f_i and d_i (i =1, 2,..., 6) are local-axis joint forces and deformations, respectively. The parameters r_j, t_j and n_j (j =1, 2) in Figure 6(b) are the so-called bending, shearing and axial stiffness degradation factors of the compound element. The factors r_j are calculated through Eq. (12), while t_j and n_j are similarly found as,

$$t_j = \frac{t_{cj}t_{pj}}{t_{cj}+t_{pj}-t_{cj}t_{pj}}; \qquad n_j = \frac{n_{cj}n_{pj}}{n_{cj}+n_{pj}-n_{cj}n_{pj}} \tag{15a, b}$$

Based on the compound model shown in Figure 6(b), the local stiffness matrix $\boldsymbol{k}$ for each element is derived accounting for the effects of shear deformation and geometrical nonlinearity. The local element stiffness matrices are transformed into the global coordinate system and then assembled as the structure stiffness matrix $\boldsymbol{K}$. If $\boldsymbol{K}$ is nonsingular at the end of an incremental load step, the corresponding incremental nodal displacements $\Delta\boldsymbol{u}$ are solved for and the incremental member-end forces $\Delta\boldsymbol{f}$ and deformations $\Delta\boldsymbol{d}$ are found. After each load step i, the total nodal displacements $\boldsymbol{u} = \Sigma\Delta\boldsymbol{u_i}$ and member-end forces $\boldsymbol{f} = \Sigma\Delta\boldsymbol{f_i}$ and deformations $\boldsymbol{d} = \Sigma\Delta\boldsymbol{d_i}$ accumulated thus far over the load history are found. The initial-yield and full-yield conditions for each member-end section are checked to detect plastic behaviour, and the corresponding bending, shearing and axial stiffness degradation factors are found. The degraded stiffnesses R_c, T_c, N_c are determined based on the moments, shear and axial forces given by the analysis results at the current loading level. The degradation factors (r_p, t_p, n_p, r_c, t_c, n_c) are applied to modify the element stiffness matrices $\boldsymbol{k}$ and, hence, the structure stiffness matrix $\boldsymbol{K}$, before commencing the next load step. The incremental-load analysis procedure continues until either a specified load level $\boldsymbol{F}$ is reached or the structure stiffness matrix $\boldsymbol{K}$ becomes singular at a lower load level as a consequence of failure of part or all of the structure. (If the structure has not failed at load level $\boldsymbol{F}$, the analysis may be continued beyond that level until failure of the structure does occur.)

The final analysis results include the values of the bending, shearing and axial post-elastic compound stiffness degradation factors r, t and n indicating the extent of plastic and connection deformation in the beam-to-column connection regions. Further computational details are provided through the analysis example presented in the following section.

5 Portal Frame Example

To illustrate and verify the proposed method it is applied to the portal frame shown in Figure 8, for which experimental test results are available in the literature (Liew *et al* 1997). In the analysis, Young's modulus E = 200 GPa and shear rigidity G = 77 GPa. Residual stress in the members for bending and axial behaviour is taken as $\sigma_r = 0.3\sigma_y$, while for shearing behaviour $\tau_r = 0.05\tau_y$, where σ_y and τ_y are respectively the normal and shearing yield stresses for steel. From the published test data (Liew *et al* 1997), the properties of the beam are: cross-section area A = 4740 mm^2, moment of inertia $I = 5547\times10^4$ mm^4, plastic modulus $Z = 485\times10^3$ mm^3, normal yield stress σ_y = 345 MPa, and shear yield stress τ_y = 199 MPa (based on von Mises criterion). The properties for both of the columns are: area A = 7600 mm^2, moment of inertia $I = 6103\times10^4$ mm^4, plastic modulus $Z = 654\times10^3$ mm^3, and yield stresses σ_y = 336 MPa and τ_y = 194 MPa. Semirigid connections are modeled by the adopted four-parameter model (Richard *et al* 1975), for which the parameter values are obtained from the test results as described in the following. Upon applying a curve-fitting technique (Liu 2005) to the moment-rotation test results for the beam-to-column connection C1 (Liew *et al* 1997), the model parameters in Eq. (6) were determined to be M_0 = 79 kN-m, R_{ce} = 7202 kN-m/rad, R_{cp} = 144 kN-m/rad, and γ = 0.57; similarly, for the column-to-base connection C2, the model parameters were determined to be M_0 = 148 kN-m, R_{ce} = 24721 kN-m/rad, R_{cp} = 151 kN-m/rad, and γ = 0.78.

To match with the experimental test setup, the loads for the analysis procedure proposed by this study are monotonically increased up to the collapse load level by incrementally changing the magnitude of the load parameter H, while maintaining the fixed proportional coefficients on the horizontal and vertical loads shown in Figure 8. The beam is divided into three elements, while each column is taken as one element. The load-deflection behaviour of joint 6 was found by the analysis to be as given by Curve 1 in Figure 9(a). Also shown in Figure 9(a) are the test results (Liew *et al* 1997) and those found using a refined plastic hinge (PHINGE) analysis method (Chen *et al* 1996). It can be seen that at lower loading levels (H < 60 kN), the load-deflection results found by this study and PHINGE method are in good agreement with each other and those obtained in the test. At higher loading levels, the results of the current study are slightly less than those of the PHINGE method because the latter does not account for elastic shear deformation as herein. Note that the results obtained by both analysis methods are significantly less than the test results at higher load levels. The proposed method predicted structure collapse at load level H_c = 74 kN, which is close to the value of 77 kN predicted by the PHINGE method, but both of these values are considerably less than the 99 kN value found as the limit load by the experimental test.

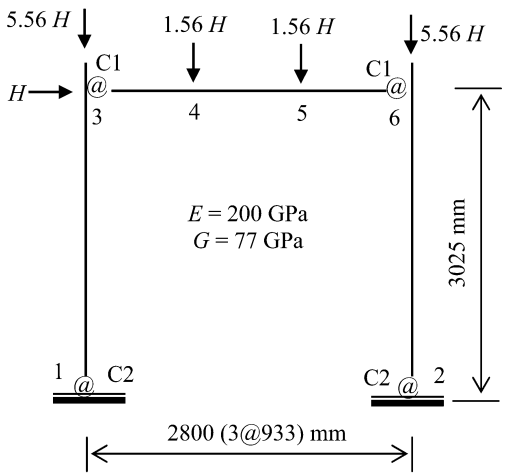

Figure 8. Tested semirigid portal frame

It likely that the above noted discrepancy between experimental and analytical results is a consequence of the analysis methods adopting connection behaviour data determined from separate pilot experiments (Liew *et al* 1997) that is different from that for the actual connections in the frame itself. In fact, a good prediction compared to the test results is found by adjusting the data for the beam-to-column connection C1 to be: M_0 = 111 kN-m, R_{ce} = 4629 kN-m/rad, R_{cp} = 1099 kN-m/rad, and γ = 0.97. The proposed analysis procedure then finds the load-deflection behaviour of joint 6 to be as defined by Curve 2 in Figure 9(a), which is observed to be in very good agreement with the experimental test results. The plastic behaviour shown in Figure 9(b) corresponds to Curve 2 in Figure 9(a). It is seen that the development of plasticity at member ends is not very significant. This is because the connections C1 and C2 respectively have ultimate moment capacities M_u = 133 kN-m and M_u = 151 kN-m, which are not that much greater than the yield moment capacities M_y = 100 kN-m and M_y = 134 kN-m of the beam and columns, respectively. In essence, the behaviour of the portal frame is governed by semi-rigid connection behaviour rather than member plasticity.

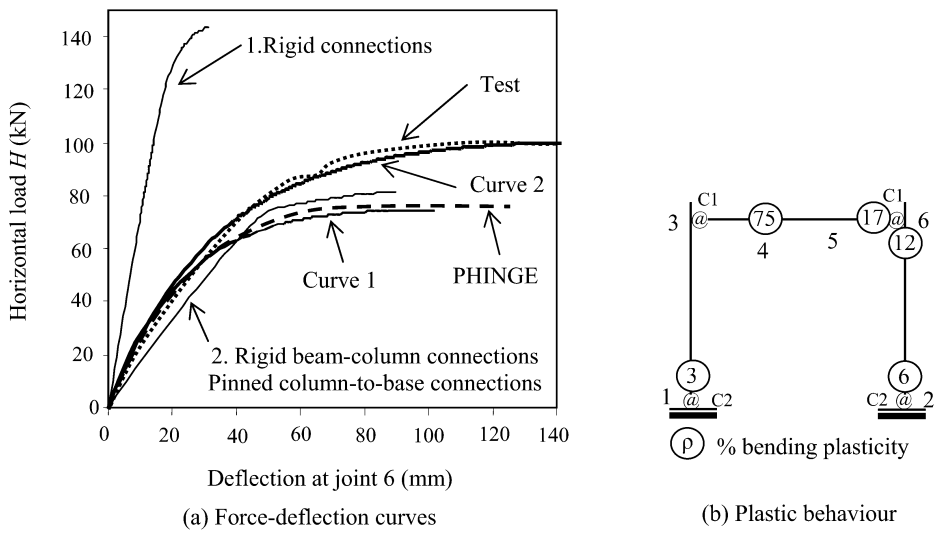

Figure 9. Load-deflection and plasticity formation

Also shown in Figure 9(a) are two special cases where the portal frame was analyzed taking some or all of the connections to be rigid. For Case 1 when both the beam-to-column and beam-to-base connections were taken to be rigid, it can be observed from the corresponding load-deflection behaviour that the limit deflection is only about one-fifth of that found for the case of semi-rigid connections, at a limit load level H_f = 143.3 kN. For Case 2 when the beam-to-column connections were assumed rigid while the column-to-base connections were taken to be pinned, which is a conventional situation in design, the corresponding load-deflection behaviour is close to that when the connections are all semi-rigid, with a frame limit load capacity H_f = 82.4 kN. The post-elastic behaviour of the frame at the limit state for the two cases is shown in Figure 10. From Figure 10(a) for the case of all rigid connections, four plastic hinges (i.e., 100% plasticity) form in the beam and right column, while the left column base undergoes 52% plasticity under combined axial force and bending moment. The formation of the fourth plastic hinge at node 4 occurs when the horizontal load H_f = 143.3 kN. At the same time, the frame fails due to inelastic instability signaled by the horizontal displacement of node 6 becoming infinitely large (i.e., the corresponding stiffness coefficient tends to zero and causes the structure stiffness matrix to become singular). From Figure 10(b) for the case of beam-to-column rigid connections and column-to-base pinned connections, the beam experiences more serious plastic deformation than the columns. The formation of the plastic hinge at the right end

of the beam occurs when the horizontal load reaches H= 77.7 kN. At limit load level H_f = 82.4 kN, the frame fails due to inelastic instability signaled by the horizontal displacement of node 6 becoming infinitely large (i.e., the same failure mode as for the rigid frame). Table 1 indicates the different degrees of member-end stiffness degradation for the scenarios when all connections are semi-rigid and the two cases where all or some of the connections are rigid.

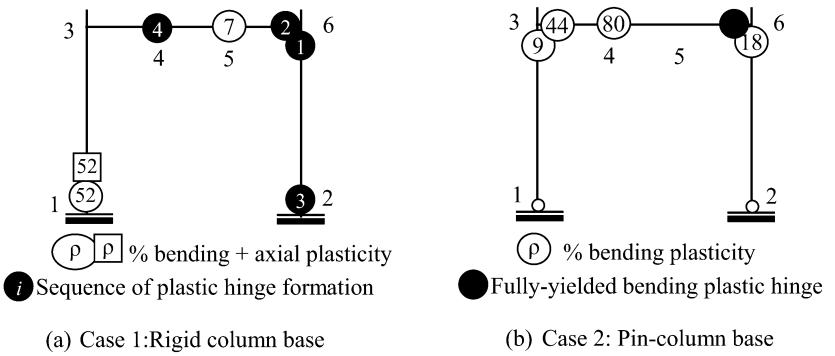

(a) Case 1:Rigid column base (b) Case 2: Pin-column base

Figure 10. Post-elastic behaviour of the rigid frame with different supports

Table 1. Stiffness degradation factors

Member	End	Semirigid				Rigid	
		Initial: r_{c0}	r_c	r_p	r	Case 1: r	Case 2: r
C13	E1	0.671	0.051	0.966	0.051	0.482	-
C26	E2	0.671	0.049	0.943	0.049	0.000	-
B34	E3	0.115	0.051	1.000	0.051	1.000	0.572
B56	E6	0.115	0.043	0.829	0.043	0.000	0.000

6 Summary and Conclusions

This article has presented a method of nonlinear analysis based on a compound-element that accounts for both member plasticity and semi-rigid connection behaviour. Depending on the properties of the compound element, connections can be categorized as being over-strength as for conventional fully-restrained or rigid connections, intermediate-strength as for partially-restrained or semi-rigid connections, and under-strength as for simple or pinned connections. Analysis results show that for an over-strength connection, both plasticity of the member and the semi-rigid nature of the connection affect nonlinear behaviour but the member strength dominates the failure state. An intermediate-strength connection has similar nonlinear behaviour but the connection strength dominates the failure state. For an under-strength connection, only the semi-rigid connection affects the nonlinear behaviour and the connection strength controls the failure state. Over-strength connections may be inappropriate for use in practice since their stiffness and strength are not fully utilized. A satisfactory design can be achieved if the connection and the connected member have about the same loading capacity.

A portal frame example demonstrated that the proposed method of nonlinear analysis can well predict the responses of structures with semirigid connections. Albeit, it was observed that the results are very dependent on properly modelling the behaviour of semi-rigid connections and that data from isolated connection tests may not be correct for assembled frameworks. The results show that the proposed method is effective and efficient for nonlinear analysis of steel frameworks taking into account flexural, shearing and axial stiffness degradation due to the combined action of member plasticity and semi-rigid connection behaviour.

Acknowledgements

This work forms part of the PhD research studies conducted by the first author under the supervision of the other two authors, and was funded by research grants from the Natural Science and Engineering Research Council of Canada.

References

AISC (American Institute of Steel Construction). (2001). *Manual of Steel Construction-Load and Resistance Factor Design* (LRFD), 3rd Edition, Chicago, Illinois.

Bjorhovde, R., Brozzeti, J., and Colson, A. (1990). "A classification system for beam to column connections." *J. Struc. Engrg*, ASCE, 116(11), 3059-3076.

CISC (Canadian Institution of Steel Construction). (2004). *Handbook of Steel Construction*. 8th Ed., Universal Offset Limited Alliston, Ontario, Canada.

Grierson, D.E., Xu, L., and Liu, Y. (2005). Progressive-failure analysis of buildings subjected to abnormal loading, *Journal of Computer-Aided Civil and Infrastructure Engineering*, **20**(3), 155-171.

Kishi, N. and Chen, W.F. (1987). *Moment-Rotation of Semi-Rigid Connections*. Structural Engineering Report, No. CE-STR-87-29, School of Civil Engineering, Purdue University, West Lafayette, Indiana.

Kishi, N., Komuro, M., and Chen, W.F. (2004). Four-parameter power model for M-θr curves of end-plate connections, ECCS/AISC Workshop Connections in Steel Structures V: Innovative Steel Connections, June, Amsterdam, The Netherlands.

Liew, J.Y.W., Yu, C.H., Ng, Y.H., and Shanmugam, N.E. (1997). Testing of semi-rigid unbraced frame for calibration of second-order inelastic analysis, *J. Construct. Steel Res*. **41**(2/3): 159-195.

Liu Y. (2006). Failure analysis of building structures under abnormal loads, *Ph.D. Thesis*, University of Waterloo, Ontario, Canada. (in progress)

Monforton, G.R. and Wu, T.S. (1963). Matrix analysis of semi-rigid connected frames, *J. Struct. Div.*, **89**(6):, 13-42.

Richard, R.M. and Abbott, B.J. (1975). Versatile elastic-plastic stress-strain formula, *J. Engrg. Mech. Div.*, ASCE, **101**(4): 511-515.

Xu, L. (1994). Optimal design of steel frameworks with semi-rigid connection. *Ph.D. Thesis*, Department of Civil Engineering, University of Waterloo, ON, Canada.

Xu, L., Liu, Y., and Grierson, D.E. (2005). Nonlinear analysis of steel frameworks through direct modification of member stiffness properties, *Advances in Engineering Software*, **36**(5): 312-324.

Yau, C.Y. and Chan, S.L. (1994). Inelastic and stability analysis of flexible connected steel frames by spring-in-series model, *J. Struct. Eng.*, ASCE, **120**(10): 2803-2819.

Ziemian, R.D., McGuire, W., and Deierlein, G.G. (1992). Inelastic limit states design Part I: Planar frame structures, *J. Struct. Engrg.*, ASCE, **118**(9): 2532-2549.